

Enhancing the performance of quantum battery by squeezing reservoir engineering

Yue Li(李月), Rong-Fang Liu(刘蓉芳), Jia-Bin You(游佳斌), Wan-Li Yang(杨万里), and Hua Guan(管桦)
Citation: Chin. Phys. B, 2026, 35 (**1**): 010303. DOI: 10.1088/1674-1056/ae1df2
http://cpb.iphy.ac.cn; http://iopscience.iop.org/cpb

What follows is a list of articles you may be interested in

Adiabatic holonomic quantum computation in decoherence-free subspaces with two-body interaction

Xiaoyu Sun(孙晓雨), Lei Qiao(乔雷), and Peizi Zhao(赵培芘)
Chin. Phys. B, 2025, 34 (**9**): 090308. DOI: 10.1088/1674-1056/adeb5e

Bayesian phase difference estimation based on single-photon projective measurement

Xu-Hao Yu(余旭豪), Ying Wei(韦颖), Ran Yang(杨然), Wen-Hui Song(宋文慧), Yingning Miao(缪应宁), Wei Zhou(周唯), Xinhui Li(李新慧), Xiaoqin Gao(高小钦), Yan-Xiao Gong(龚彦晓), and Shi-Ning Zhu(祝世宁)
Chin. Phys. B, 2025, 34 (**7**): 070305. DOI: 10.1088/1674-1056/adde33

Correcting on-chip distortion of control pulses with silicon spin qubits

Ming Ni(倪铭), Rong-Long Ma(马荣龙), Zhen-Zhen Kong(孔真真), Ning Chu(楚凝), Wei-Zhu Liao(廖伟筑), Sheng-Kai Zhu(祝圣凯), Chu Wang(王储), Gang Luo(罗刚), Di Liu(刘峘), Gang Cao(曹刚), Gui-Lei Wang(王桂磊), Hai-Ou Li(李海欧), and Guo-Ping Guo(郭国平)
Chin. Phys. B, 2025, 34 (**1**): 010308. DOI: 10.1088/1674-1056/ad8db1

Established conversions for hybrid entangled states assisted by error-predicted parity-discriminated devices

Fang-Fang Du(杜芳芳), Zhi-Guo Fan(范志国), Xue-Mei Ren(任雪梅), Ming Ma(马明), and Wen-Yao Liu(刘文耀)
Chin. Phys. B, 2025, 34 (**1**): 010303. DOI: 10.1088/1674-1056/ad8fa0

Coupling and characterization of a Si/SiGe triple quantum dot array with a microwave resonator

Shun-Li Jiang(江顺利), Tian-Yi Jiang(蒋天翼), Yong-Qiang Xu(徐永强), Rui Wu(吴睿), Tian-Yue Hao(郝天岳), Shu-Kun Ye(叶澍坤), Ran-Ran Cai(蔡冉冉), Bao-Chuan Wang(王保传), Hai-Ou Li(李海欧), Gang Cao(曹刚), and Guo-Ping Guo(郭国平)
Chin. Phys. B, 2024, 33 (**9**): 090311. DOI: 10.1088/1674-1056/ad711d

---

RAPID COMMUNICATION

Enhancing the performance of quantum battery by squeezing reservoir engineering

Yue Li(李月)[1,2], Rong-Fang Liu(刘蓉芳)[1,3], Jia-Bin You(游佳斌)[4,5,†], Wan-Li Yang(杨万里)[1,‡], and Hua Guan(管桦)[1]

[1] *State Key Laboratory of Magnetic Resonance and Atomic and Molecular Physics, Innovation Academy for Precision Measurement Science and Technology, Chinese Academy of Sciences, Wuhan* 430071, *China*

[2] *School of Physical Sciences, University of Chinese Academy of Sciences, Beijing* 100049, *China*

[3] *Key Laboratory of Quantum Theory and Applications of MoE, Lanzhou Center for Theoretical Physics, and Key Laboratory of Theoretical Physics of Gansu Province, Lanzhou University, Lanzhou* 730000, *China*

[4] *Quantum Innovation Centre (Q.InC), Agency for Science, Technology and Research (A*STAR), Singapore* 138634, *Republic of Singapore*

[5] *Institute of High Performance Computing (IHPC), Agency for Science, Technology and Research (A*STAR), Singapore* 138632, *Republic of Singapore*

(Received 22 October 2025; revised manuscript received 6 November 2025; accepted manuscript online 11 November 2025)

Reservoir engineering has been widely used in various quantum technologies. Based on a cavity-QED (quantum electrodynamics) model, we propose a potentially practical scheme using squeezed-vacuum reservoir engineering to optimize the performance of a quantum battery (QB) located inside a cavity driven by a broadband squeezed laser, which acts as a squeezed-vacuum reservoir. Using the reduced master equation of the QB obtained via the adiabatic elimination method, we focus on the QB's charging dynamics under tunable squeezed reservoirs governed by parametrically controlled squeezing parameters, which dictate the efficiency of energy transfer and the extractable work (ergotropy) of the QB. We show that increasing the squeezing strength improves the charging rate and enables rapid energy transfer, whereas the steady-state energy of the QB saturates at specific values of the squeezing parameter. Notably, the ergotropy of the QB reaches its maximum at a critical squeezing strength and does not scale monotonically with the squeezing strength. This nonmonotonic behavior underscores the existence of optimal parameter regimes, through which the performance of the QB can be significantly enhanced.

Keywords: quantum computation, cavity quantum electrodynamics

PACS: 03.67.Lx, 42.50.Pq

DOI: 10.1088/1674-1056/ae1df2 **CSTR:** 32038.14.CPB.ae1df2

1. Introduction

Beyond their conventional role as quantum registers or memories in quantum information processing, quantum systems can also be excited by external chargers or drives to serve as energy reservoirs, whose stored energy may subsequently be released in a controllable manner during unitary operation cycles. It is within this framework that the research field of quantum batteries (QBs) emerges.[1–7] In brief, QBs offer potential advantages over classical counterparts, including enhanced energy storage density in large-scale integrations and accelerated charging rates. Recent investigations have highlighted the critical role of different quantum resources in optimizing QB performance,[8–21] such as improving work extraction — quantified via ergotropy, a measure of maximal work extraction under cyclic unitary operations,[22–26] charging power,[27–31] and energy storage stability.[32–34] Experimentally, QBs have been simulated in diverse platforms,[35–45] including organic semiconductors coupled to microcavities,[35] semiconductor quantum dots embedded in optical microcavities,[36] superconducting-qubit systems,[39,40,46] and linear optical systems.[41–43] Recent experimental progress has realized the charging process of QBs through distinct quantum control methods: indefinite causal-order implementation in linear optical systems,[43] interference-based control using emitted fields and coherent laser fields,[44] and measurement-feedback approaches via single-ion information engines.[45] These advancements provide foundational insights into QB realization.

On the other hand, quantum squeezing enables the reduction of variance in one quantum-mechanical quadrature below the standard quantum limit, a property leveraged in recent developments in QBs. Recent investigations into QB protocols highlight the role of squeezing effects in enhancing the charging dynamics of QBs.[21,47–52] Reference [21] demonstrates that a QB subjected to a strongly squeezed drive and an incoherent squeezed thermal reservoir exhibits enhanced thermodynamic efficiency. Concurrently, Downing and Ukhtary[50] circumvent energy leakage in QBs by exploiting quadratic driving with short temporal pulses. This protocol induces hyperbolic enhancement of stored energy, scaling with the square

[†]Corresponding author. E-mail: you_jiabin@a-star.edu.sg

[‡]Corresponding author. E-mail: ywl@wipm.ac.cn

© 2026 Chinese Physical Society and IOP Publishing Ltd. All rights, including for text and data mining, AI training, and similar technologies, are reserved.

of the pulse amplitude. Notably, such quadratic driving generates significant useful work near critical points of dissipative phase transitions.[49]

While these results indicate the potential of quantum squeezing for QBs, the pursuit of high-efficiency energy storage and fast charging motivates exploration of new protocols to further enhance charging power and energetic efficiency. Reservoir engineering (the deliberate design of system-reservoir couplings to achieve specific quantum states and dynamics) has emerged as a promising avenue due to its capacity for coherence control.[53–56] In particular, squeezed-vacuum reservoir engineering has enabled advances in various quantum information tasks, including high-efficiency measurement,[57,58] entanglement distribution and generation,[59–62] spin squeezing,[63] unique resonance fluorescence spectra,[64,65] and squeezing or cooling of mechanical resonators.[66] Inspired by these advances, we propose an experimental platform employing squeezed-reservoir engineering to optimize QB performance. The QB, embedded in an optical cavity, is driven by a broadband squeezed laser acting as a squeezed-vacuum reservoir. Using the adiabatic elimination method[67,68] in the bad-cavity limit, we derive a reduced master equation to study charging dynamics. We quantitatively characterize stored energy and ergotropy (extractable work) as functions of the squeezing parameters. Our analysis reveals that increasing the squeezing strength accelerates energy transfer rates during charging. However, the steady-state energy saturates beyond a critical squeezing parameter due to competition between nonlinear interactions and dissipative effects. Crucially, the ergotropy displays a nonmonotonic dependence on the squeezing strength, reaching its maximum at an optimal squeezing parameter. This demonstrates a fundamental trade-off: while stronger squeezing enhances charging speed, it may conversely reduce work-extraction efficiency. Therefore, tailored squeezing protocols can maximize overall QB performance by mitigating energetic losses at the expense of reduced ergotropy, establishing optimal squeezing parameter regimes for QB enhancement.

The paper is organized as follows. In Section 2 we give a brief introduction of the model and the figures of merit that we will be mainly interested in throughout this work. Section 3 describes the performance of QBs under different parameter conditions. We discuss and conclude in Section 4.

2. Model and method

Consider a cavity-QED (quantum electrodynamics) system in which two independent qubits are confined in a single-mode cavity driven by an external laser field, as schematically represented in Fig. 1. In the rotating frame with $H_{\rm c} = \omega_{\rm L} c^\dagger c + \frac{\omega_{\rm L}}{2}\sum_j \sigma_j^z$, the Hamiltonian of the whole system can be expressed as ($\hbar = 1$)

$$H = \Delta_c c^\dagger c + \sum_j^2 \left[\frac{\Delta_a}{2}\sigma_j^z + g_j(c^\dagger \sigma_j^- + c\sigma_j^+)\right] + \Omega(c^\dagger + c). \quad (1)$$

The annihilation and creation operators for the cavity field are represented by c and $c^\dagger$, and the operators for the qubits operating at the same frequency ω_0 are denoted by σ_j^α (where $\alpha = z, \pm$). The coupling strength between the cavity field and the j-th qubit is indicated by the parameter g_j. The detunings are defined as follows: $\Delta_{\rm c} = \omega_{\rm c} - \omega_{\rm L}$, $\Delta_a = \omega_0 - \omega_{\rm L}$, representing the differences between the laser frequency $\omega_{\rm L}$ and the cavity frequency $\omega_{\rm c}$ or qubit transition frequency ω_0, respectively. $\Omega = 2\sqrt{p\kappa/\omega_{\rm L}}$ provides the driving amplitude, where p is the input laser power and κ is the cavity damping rate.

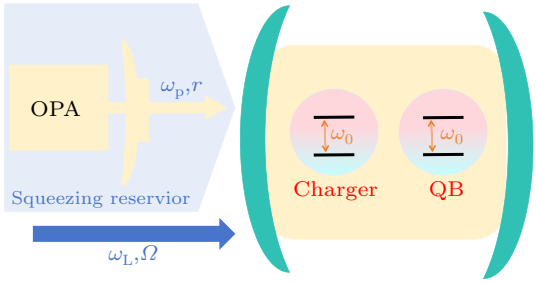


Fig. 1. Schematic of the squeezing QB setup: a cavity-QED system consisting of a pair of qubits (QB and charger), driven by a coherent laser with frequency $\omega_{\rm L}$ and driving amplitude Ω. A broadband squeezed laser field, generated by an OPA with squeezing degree r around the central frequency $\omega_{\rm p}$, is injected into the cavity.

In the present model, the cavity is driven by a broadband squeezed laser field, which is generated by an optical parametric amplifier (OPA) and is characterized by a squeezing degree r and a central frequency $\omega_{\rm p}$. This cavity field, in turn, acts as a squeezed-vacuum reservoir for the qubits, constituting the main point of our squeezed-reservoir engineering. Taking all these dissipative effects into account and under the Born–Markovian approximation, we can derive a master equation for the density matrix $\rho_{ac}(t)$ of the total system consisting of the cavity field and the qubits as

$$\dot{\rho}_{ac}(t) = -{\rm i}[H, \rho_{ac}(t)] + \mathcal{L}_a \rho_{ac}(t) + \mathcal{L}_{\rm c}\rho_{ac}(t). \quad (2)$$

The dissipation effects with respect to the qubits and cavity can be described by the Lindblad superoperator terms $\mathcal{L}_a = \sum_j \gamma_j \check{\mathcal{D}}_{\sigma_j^-, \sigma_j^+}$ and $\mathcal{L}_{\rm c} = \kappa(N+1)\check{\mathcal{D}}_{c,c^\dagger} + \kappa N \check{\mathcal{D}}_{c^\dagger,c} - \kappa[M{\rm e}^{2{\rm i}\Delta_{\rm p}t}\check{\mathcal{D}}_{c,c} + {\rm h.c.}]$, respectively. Here, $\Delta_{\rm p} = \omega_{\rm p} - \omega_{\rm L}$ is the detuning between the broadband squeezing driving field and the coherent driving field, while $M = \cosh r \sinh r$ and $N = \sinh^2 r$ are related to the squeezing parameter of the reservoir. γ_j and κ are the dissipation rates of the qubits and the cavity, respectively, and the superoperator $\check{\mathcal{D}}_{o,p}$ is defined as $\check{\mathcal{D}}_{o,p}\rho(t) = 2o\rho(t)p - \{po, \rho(t)\}$, which satisfies the Lindblad form.

Under the interaction picture $U = \exp({\rm i}(\Delta_{\rm c} c^\dagger c + \sum_j^2 \Delta_a \sigma_j^z/2)t)$, combined with the squeezing transformation

$\bar{\rho}_{ac}(t) = SU\rho_{ac}(t)U^{\dagger}S^{\dagger}$ with $S = \mathrm{e}^{(r(c^2-c^{\dagger 2})/2)}$, Eq. (2) can be rewritten as

$$\dot{\bar{\rho}}_{ac}(t) = -\mathrm{i}[\bar{H}_i, \bar{\rho}_{ac}(t)] + \mathcal{L}_a\bar{\rho}_{ac}(t) + \mathcal{L}_{\bar{c}}\bar{\rho}_{ac}(t), \tag{3}$$

where $\bar{H}_i = c^{\dagger}A(t) + \text{h.c.}$ and $\mathcal{L}_{\bar{c}} = \kappa\mathcal{D}_{c,c^{\dagger}}$ with $A(t) = \sum_{j=1,2}[g_j(\sigma_j^- \mathrm{e}^{\mathrm{i}(\Delta-\Delta_a)t}\sqrt{N+1} + \sigma_j^+ \mathrm{e}^{-\mathrm{i}(\Delta-\Delta_a)t}\sqrt{N}) + \Omega(t)]$ and $\Omega(t) = \Omega(\mathrm{e}^{\mathrm{i}\Delta t}\sqrt{N+1} + \mathrm{e}^{-\mathrm{i}\Delta t}\sqrt{N})$. Here, we set $\Delta_{\mathrm{c}} = \Delta_{\mathrm{p}} = \Delta$.

Based on the adiabatic elimination method,[61,69,70] the cavity field can be eliminated in the limit of $\kappa \gg \gamma_j$. Under the Born approximation, $\rho_{ac}(t)$ can be factorized as $\rho_{ac}(t) \approx \rho_a(t) \otimes (|0\rangle\langle 0|_{\mathrm{c}})$, yielding a reduced master equation for the two qubits with $\tilde{\rho}(t) = \mathrm{Tr}_{\mathrm{c}}[\tilde{\rho}_{ac}(t)]$. For this purpose, we rewrite Eq. (3) as $\tilde{\rho}_{ac}(t) = \mathrm{e}^{-\mathcal{L}_{\bar{c}}t}\bar{\rho}_{ac}(t)$, leading to

$$\begin{aligned}\dot{\tilde{\rho}}_{ac}(t) \;=\; & \mathcal{L}_a\tilde{\rho}_{ac}(t) - \mathrm{i}A(t)\,\mathrm{e}^{-\mathcal{L}_{\bar{c}}t}[\bar{\rho}_{ac}(t)c^{\dagger}] \\ & + \mathrm{i}\,\mathrm{e}^{-\mathcal{L}_{\bar{c}}t}[c\bar{\rho}_{ac}(t)]A^{\dagger}(t) - \mathrm{i}A^{\dagger}(t)\,\mathrm{e}^{-\mathcal{L}_{\bar{c}}t}[c\bar{\rho}_{ac}(t)] \\ & + \mathrm{i}\,\mathrm{e}^{-\mathcal{L}_{\bar{c}}t}[\bar{\rho}_{ac}(t)c^{\dagger}]A(t) - \mathrm{i}A(t)e^{-\mathcal{L}_{\bar{c}}t}[c^{\dagger},\bar{\rho}_{ac}(t)] \\ & - \mathrm{i}\,\mathrm{e}^{-\mathcal{L}_{\bar{c}}t}[c,\bar{\rho}_{ac}(t)]A^{\dagger}(t),\end{aligned} \tag{4}$$

where

$$\begin{aligned}&\mathrm{e}^{-\mathcal{L}_{\bar{c}}t}[c^{\dagger},\bar{\rho}_{ac}(t)] = \mathrm{e}^{\kappa t}[c^{\dagger},\tilde{\rho}_{ac}(t)], \\ &\mathrm{e}^{-\mathcal{L}_{\bar{c}}t}[c,\bar{\rho}_{ac}(t)] = \mathrm{e}^{\kappa t}[c,\tilde{\rho}_{ac}(t)], \\ &\mathrm{e}^{-\mathcal{L}_{\bar{c}}t}[c\bar{\rho}_{ac}(t)] = \mathrm{e}^{-\kappa t}c\tilde{\rho}_{ac}(t), \\ &\mathrm{e}^{-\mathcal{L}_{\bar{c}}t}[\bar{\rho}_{ac}(t)c^{\dagger}] = \mathrm{e}^{-\kappa t}\tilde{\rho}_{ac}(t)c^{\dagger}.\end{aligned} \tag{5}$$

Taking $t' = t - \tau$ and tracing over the cavity degrees of freedom, we obtain the reduced master equation for the two qubits

$$\begin{aligned}\dot{\tilde{\rho}} \;=\; & \mathcal{L}_a\tilde{\rho}(t) + \int_0^{\infty}\mathrm{e}^{-\kappa t}[A(t)\tilde{\rho}(t)A^{\dagger}(t-\tau) \\ & - A^{\dagger}(t)A(t-\tau)\tilde{\rho}(t) + \text{h.c.}]\,\mathrm{d}\tau.\end{aligned} \tag{6}$$

Returning to the Schrödinger picture, the reduced master equation for the two qubits becomes

$$\begin{aligned}\dot{\rho}(t) \;=\; & -\mathrm{i}[H_0,\rho(t)] + \mathcal{L}_a\rho(t) \\ & + \Bigg\{\sum_{j,k}^{2} g_jg_k\Big[\Omega K\sum_{j=1,2}g_j[\rho(t),\sigma_j^+] \\ & + \mathrm{e}^{-2\mathrm{i}\Delta t}FM(2\sigma_j^+\rho(t)\sigma_k^+ - \rho(t)\sigma_k^+\sigma_j^+ - \sigma_j^+\sigma_k^+\rho(t))\Big] \\ & + NF(\sigma_j^-\rho(t)\sigma_k^+ - \rho(t)\sigma_k^+\sigma_j^- + \sigma_k^+\rho(t)\sigma_j^- \\ & - \sigma_j^-\sigma_k^+\rho(t)) + F\left[\sigma_j^-\rho(t)\sigma_k^+ - \rho(t)\sigma_k^+\sigma_j^-\right] + \text{h.c.}\Bigg\},\end{aligned} \tag{7}$$

where $H_0 = \Delta_a\sum_j\sigma_j^z/2$, $F = \frac{1}{\kappa-\mathrm{i}(\Delta-\Delta_a)}$, and $K = \frac{1}{\kappa+\mathrm{i}\Delta}$.

3. The performance of QB

Assuming that the first qubit acts as the charger (denoted by C) and the second qubit serves as the quantum battery (denoted by B), the dynamics of stored energy of the QB can be expressed as

$$\Delta E_{\mathrm{B}}(t) = \mathrm{Tr}[H_{\mathrm{B}}\rho_{\mathrm{B}}(t)], \tag{8}$$

where $\rho_{\mathrm{B}}(t) = \mathrm{Tr}_C[\rho(t)]$ is the reduced density matrix of the QB. According to the second law of thermodynamics, $\Delta E_{\mathrm{B}}(t)$ cannot be fully extracted from the QB. Therefore, a suitable measure of the extractable work is introduced using the concept of ergotropy:[22–26] the maximum amount of energy that can be unitarily extracted, defined as the difference between the internal energy of the QB and that of its corresponding passive state $\tilde{\rho}_{\mathrm{B}}(t)$, which provides no energy under unitary operations:

$$\mathcal{W}(t) = \Delta E_{\mathrm{B}}(t) - \min_U \mathrm{Tr}\left[H_{\mathrm{B}}U\rho_{\mathrm{B}}(t)U^{\dagger}\right], \tag{9}$$

where the minimization is performed over all unitaries U acting locally on the QB. By diagonalizing H_{B} and $\rho_{\mathrm{B}}(t)$, one can obtain their spectral decompositions as $\rho_{\mathrm{B}}(t) = \sum_j \varepsilon_j |\varepsilon_j\rangle\langle\varepsilon_j|$ and $H_{\mathrm{B}} = \sum_j e_j |e_j\rangle\langle e_j|$. The eigenvalues of $\rho_{\mathrm{B}}(t)$ are arranged in descending order, $\varepsilon_j \geqslant \varepsilon_{j+1}$, and the eigenvalues of H_{B} in ascending order, $e_j \leqslant e_{j+1}$. The term $\min_U \mathrm{Tr}\left[H_{\mathrm{B}}U\rho_{\mathrm{B}}(t)U^{\dagger}\right]$ in Eq. (9) simplifies to $\sum_n e_n\varepsilon_n$. Another important quantity characterizing the QB's efficiency is the ratio between the extractable work and the stored energy

$$R(t) = \mathcal{W}(t)/\Delta E_{\mathrm{B}}(t). \tag{10}$$

Figure 2(a) analyzes the dynamics of stored energy $\Delta E_{\mathrm{B}}(t)$ of the QB under different squeezing conditions. In the weak squeezing regime ($0 < r < 1$), the charging efficiency remains low, and at the end of the dynamics the energy persists at minimal values below 0.04. In the moderate squeezing regime ($1 < r < 2$), the charging behavior exhibits a measurable degree of optimization, with the energy reaching its maximum value within a shorter timescale, less than 100. In summary, the high-energy region becomes broader, accompanied by a longer duration for peak-energy preservation as the squeezing strength r increases. Further increasing r into the strong squeezing regime ($r > 2$) significantly improves the charging efficiency, enabling the QB to reach its saturation value rapidly. This fast-charging process constitutes a defining feature of the strong squeezing regime, as shown explicitly in Fig. 2(a).

In Fig. 2(b), we present the dynamics of $\Delta E_{\mathrm{B}}(t)$ for different r. The energy increases over time until it reaches a saturation value, and the maximum energy increases significantly with r. In addition to this trend, each curve exhibits superimposed minor oscillations. While the energy shows a decreasing trend at the end of the dynamics when $r = 0$, this trend is absent under squeezing. These results demonstrate that squeezing effects significantly enhance the robustness of ΔE_{B} against dissipation. Under squeezing, the energy persists near its steady-state value with minimal oscillations. Notably,

the first peak appears earlier for larger r, indicating a faster charging process assisted by quantum squeezing. Specifically, $\Delta E_{\max}$ increases with r, and the time required to reach $\Delta E_{\max}$ decreases with increasing r. For instance, the orange line ($r = 1.5$) reaches its first peak at $t \approx 50$, which is one-tenth of the time $t \approx 500$ required to reach maximum energy for $r = 0$ (red line). This is because squeezing effectively enhances the QB-charger coupling, leading to faster energy exchange. The underlying mechanism is the nonclassical effects induced by squeezing, which transform the initial state, enhance quantum fluctuations and coherence, and accelerate energy transfer. Stronger squeezing results in more pronounced nonclassical effects, yielding faster charging and increased total stored energy.

Figure 3 presents the dynamics of ΔE_{B} across three parameter regimes of r: weak squeezing ($0 < r < 1$), moderate squeezing ($1 < r < 2$), and strong squeezing ($2 < r < 4$). For $0 < r < 1$ in Fig. 3(a), ΔE_{B} increases monotonically with time and then asymptotically approaches a saturation value. The maximum attainable energy $\Delta E_{\max}$ scales strongly with r. In addition to this dominant behavior, each energy evolution curve exhibits superimposed small-amplitude oscillations. When $1 < r < 2$, the main features of the four curves in Fig. 3(b) closely resemble those in Fig. 3(a). However, the characteristic time t_{c} required to reach $\Delta E_{\max}$ is further reduced, the saturation values under different r converge more closely, and the small oscillations previously observed along each curve in Fig. 3(a) nearly vanish.

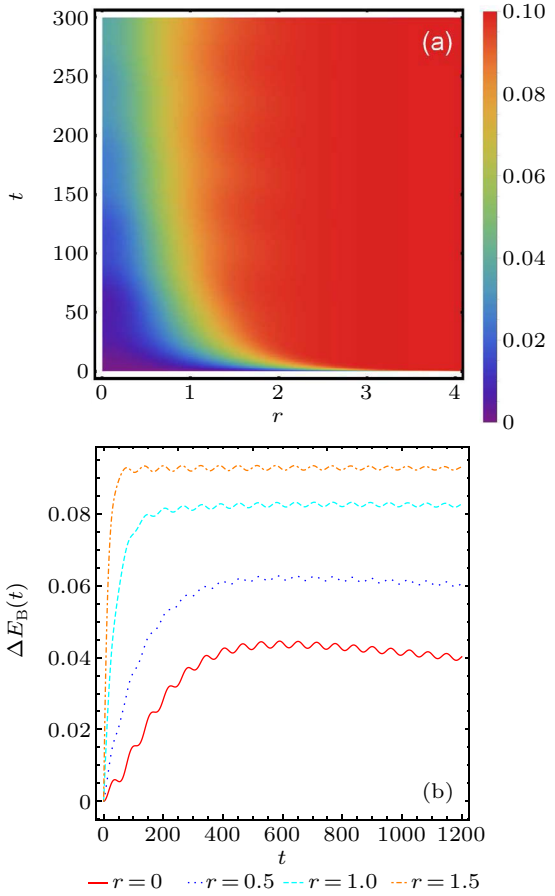


Fig. 2. (a) Stored energy $\Delta E_{\mathrm{B}}(t)$ as a function of squeezing strength r and dimensionless time t. (b) Dynamics of $\Delta E_{\mathrm{B}}(t)$ for different r, where the red, blue, cyan, and orange lines correspond to squeezing degrees $r = 0$, $r = 0.5$, $r = 1$, and $r = 1.5$, respectively. Other parameters are set as $\kappa = 0.7$, $\Omega = 0.1$, $g_1 = g_2 = 0.05$, $\omega_0 = 0.2$, $\omega_{\mathrm{c}} = 0.2$, and $\omega_{\mathrm{L}} = 0.1$.

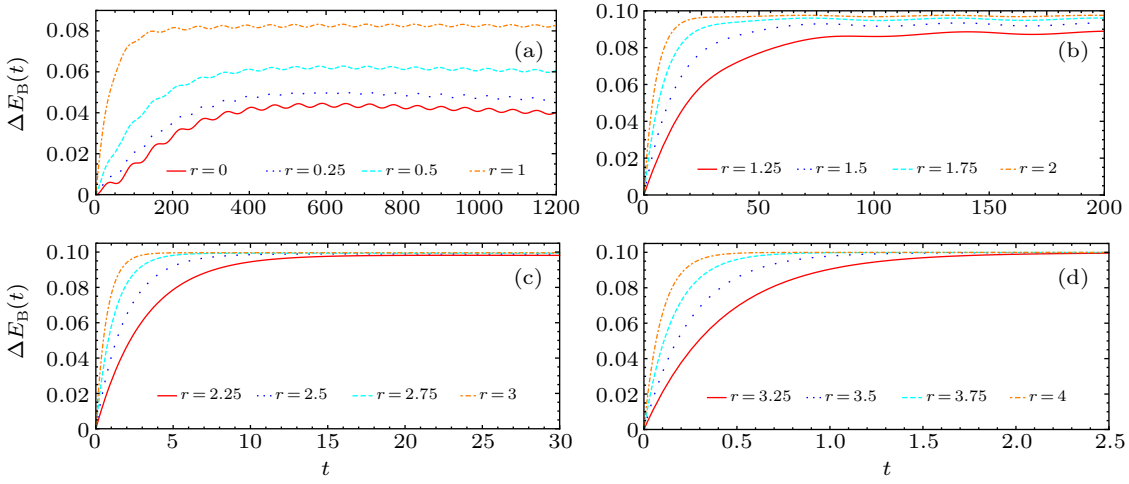


Fig. 3. Dynamics of stored energy for different squeezing parameters. Other parameters are set consistently with Fig. 2.

More notably, the strong squeezing regime ($2 < r < 4$) exhibits an ultra-fast charging rate. At $t_{\mathrm{c}} \approx 20$, ΔE_{B} rapidly saturates, and the QB achieves an ultra-fast charging process facilitated by strong quantum squeezing. Furthermore, the time t_{c} can be reduced to as low as about 2 when $r > 3$, as shown in the inset of Fig. 3(c). These behaviors reveal an r-dependent optimization of the charging time for the QB. Within an extremely short duration, the steady-state stored energy ΔE_{ss} converges, irrespective of r. Although quantum squeezing modifies the QB's state and dynamics, the ultimate steady state is determined solely by the reservoir's temperature, leading to identical steady-state energies for different values of r. This indi-

cates that, in the present model, the squeezing effect has limited impact on the long-time performance of the QB, although it drives the QB into equilibrium more rapidly. Most notably, an optimal energy exists corresponding to a critical squeezing parameter r_c. Once r_c is exceeded, ΔE_B no longer increases, although the charging time can be further reduced with increasing squeezing strength. Physically, the faster charging of the QB in the presence of squeezing arises from the squeezing-amplified effective QB-charger coupling strength, thereby increasing the energy transfer rate. These mechanisms demonstrate how squeezing parameters can strategically control the QB's performance metrics. As is well-known, a squeezing effect, rooted in Heisenberg's uncertainty principle, is defined as the reduction in the uncertainty of one observable at the cost of increased uncertainty in its conjugate.[71,72] Physically, the squeezing in the reservoir inevitably modifies the non-unitary relaxation dynamics and the associated irreversibility during the thermodynamic process.

Figure 4 illustrates how $\mathcal{W}(t)$ evolves in the parameter space of r and t. It shows that the inherent squeezing effect stemming from the reservoir plays a crucial role and significantly influences $\mathcal{W}(t)$. When $0 < r < 1.5$, $\mathcal{W}(t)$ exhibits damped oscillations toward a steady-state value, and the oscillation peaks become narrower with increasing r. Once r exceeds 1.5, the oscillation period becomes shorter, and the oscillation peaks become wider. However, the maximal value of ergotropy $\mathcal{W}_{\max}$ does not increase monotonically with increasing r, and a distinct optimal regime emerges near $r_{op} \approx 1.8$, where $\mathcal{W}(t)$ achieves the highest peak values and most favorable steady-state performance. The optimized $\mathcal{W}(t)$ in the intermediate squeezing regime ($1.5 < r < 2$) arises from the competing effects between the squeezing-enhanced energy transfer rate and the accelerated decoherence due to stronger system–reservoir coupling at large r. Simultaneously, the squeezing operation introduces additional quantum noise that amplifies the system–reservoir coupling, leading to intensified dissipation. Therefore, the optimal squeezing parameter r_{op} represents a balance point where coherent dynamics competes with dissipative losses. When $r > 3$, $\mathcal{W}(t)$ remains small during the charging process. This implies that the performance of the QB can be optimized by modulating the degree of squeezing, as shown in Fig. 4(a). Notably, increasing the squeezing strength r effectively enhances the QB–charger coupling, thereby reducing the charging time. However, once r exceeds a critical threshold, dissipative effects dominate: oscillations are suppressed, and the system rapidly equilibrates. This trade-off yields an optimal squeezing parameter $r_{op} \approx 1.8$ for peak energy storage and work extraction, where the squeezing-enhanced energy transfer and dissipation-induced losses achieve dynamical balance.

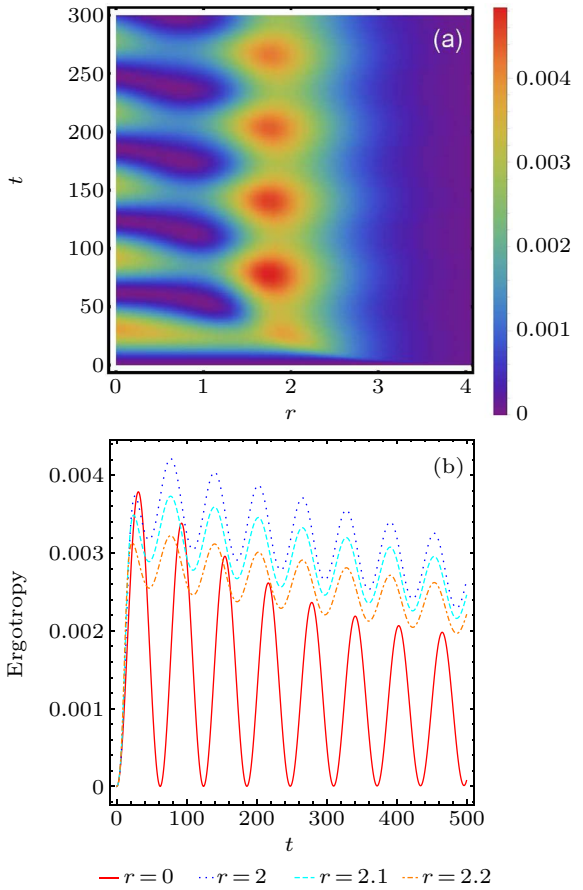


Fig. 4. (a) Ergotropy $\mathcal{W}(t)$ as a function of squeezing strength r and dimensionless time t. (b) Dynamics of ergotropy $\mathcal{W}(t)$ for different r, where the red, blue, cyan, and orange lines correspond to $r = 0$, $r = 2$, $r = 2.1$, and $r = 2.2$, respectively. Other parameters are set consistently with Fig. 2.

Figure 4(b) shows the evolution of $\mathcal{W}(t)$ for different r. In the non-squeezing case ($r = 0$), $\mathcal{W}(t)$ exhibits damped oscillations with relatively low amplitude and approaches zero periodically. Consequently, the difference $\Delta\mathcal{W}(t) = \mathcal{W}_{\max} - \mathcal{W}_{\min}$ between the maximum and minimum values of ergotropy is large. In contrast, $\Delta\mathcal{W}(t)$ gradually decreases as r increases. Note that $\mathcal{W}_{\max}$ does not grow monotonically with r, indicating the existence of an optimal squeezing parameter for work extraction and implying a trade-off between squeezing-enhanced energy transfer and decoherence-induced dissipation. At $r \approx 2.2$, decoherence dominates over coherent dynamics, driving the system into an overdamped regime.

It is important to emphasize that the trend of $\mathcal{W}(t)$ differs from that of ΔE_B. For ΔE_B, increasing the squeezing strength enables the QB to store more energy with shorter charging time, as the squeezing induces stronger QB–charger interaction and speeds up the charging process. In contrast, $\mathcal{W}(t)$ exhibits a more intricate dependence on r and does not demonstrate such pronounced advantages. To analyze this dependence in detail, we partition r into discrete intervals and examine specific values, as shown in Fig. 5.

In the weak squeezing regime ($0 < r < 1$), both the peak width and the peak value of the maximal ergotropy $\mathcal{W}_{\max}$ de-

crease with r. In the moderate squeezing regime ($1 < r < 2$), for $r > 1.5$, increasing r enhances $\mathcal{W}(t)$, with an optimal squeezing parameter $r_{\rm op} \approx 1.8$ at which $\mathcal{W}_{\rm max}$ reaches its maximum. In the strong squeezing regime ($2 < r < 3$), only the red curve ($r = 2.25$) shows an advantage over the case of $r = 0$, while other curves exhibit no observable benefits except for their non-vanishing amplitudes in the long-time limit. In the ultra-strong squeezing regime ($r > 3$), $\mathcal{W}(t)$ remains persistently low, significantly below the values observed in the absence of quantum squeezing.

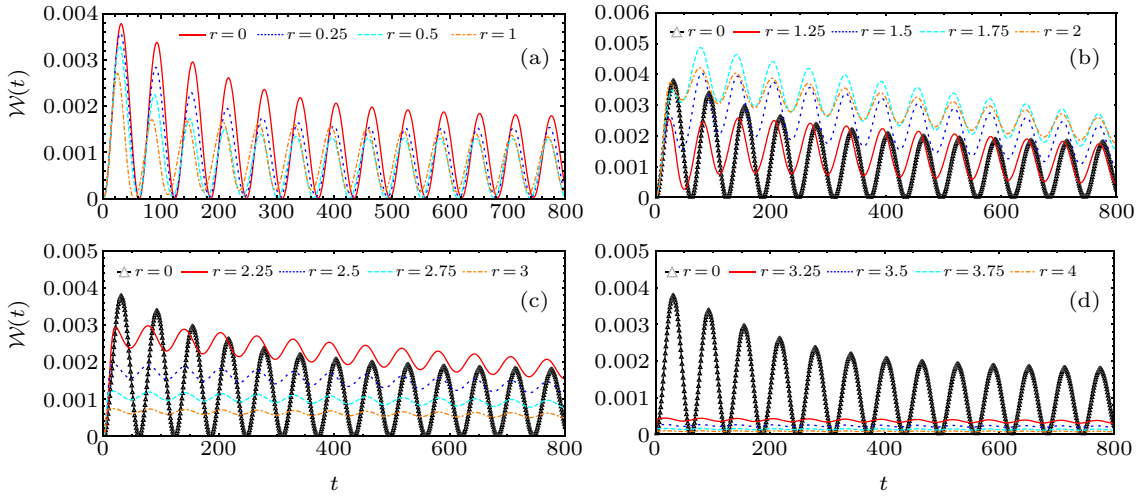


Fig. 5. Dynamics of ergotropy $\mathcal{W}(t)$ for different squeezing parameters. Other parameter settings are consistent with Fig. 2.

Therefore, from the perspective of quantum reservoir engineering, employing a squeezed reservoir represents a promising approach for utilizing the squeezing effect as a quantum resource to enhance the performance of a QB. However, strong squeezing simultaneously amplifies dissipation. Consequently, achieving optimal QB performance requires precise engineering of the squeezing strength parameter with high accuracy.

4. Discussion and conclusion

Compared to the model in Ref. [21], which employs an incoherent squeezed thermal bath, our scheme utilizes a broadband squeezed laser to engineer a squeezed-vacuum reservoir for the cavity-QED system, enabling dynamic control over both coherent and dissipative processes. While Ref. [50] demonstrates hyperbolic energy enhancement via pulsed quadratic driving, our work employs continuous-wave squeezing, facilitating a stable steady-state analysis and revealing a nonmonotonic behavior of ergotropy with respect to the squeezing strength — a crucial trade-off not highlighted in their transient pulse scheme. In contrast to Ref. [49], which focuses on critical phenomena near dissipative phase transitions in a quadratically driven system, our work explores the full parameter space of squeezing strength, identifying distinct charging regimes (weak, moderate, and strong squeezing) and an optimal squeezing parameter for maximal ergotropy. Therefore, our work identifies a fundamental trade-off between squeezing-enhanced charging and ergotropy degradation beyond a critical squeezing strength, a phenomenon previously unaddressed in the literature.[21,49,50]

While our analysis is based on a Markovian framework, incorporating non-Markovian effects could offer further avenues for performance optimization in our squeezed-reservoir QB model.[11,73–77] Non-Markovian environments, characterized by memory effects and information backflow, may allow partial recovery of energy otherwise lost to the reservoir. In the present model, such memory effects could potentially reinforce squeezing-enhanced coherent dynamics, mitigating the ergotropy degradation observed at high squeezing strengths. Future work could explore this prospect by integrating structured, non-Markovian reservoirs into the present cavity-QED setup.[78,79] Investigating the interplay between engineered squeezing and environmental memory could reveal new mechanisms for sustaining high ergotropy and stabilizing battery performance.

Regarding experimental feasibility, generating broadband squeezed light via optical parametric amplifiers (OPAs) or oscillators (OPOs) is a well-established technique. Crucially, injecting such squeezed fields into optical cavities to engineer the effective dissipative environment for embedded quantum emitters has been experimentally demonstrated. The seminal work demonstrated the interaction of an artificial atom (a superconducting qubit) with a squeezed vacuum field generated by a Josephson parametric amplifier (JPA).[65] The modification of the resonance fluorescence spectrum observed provides clear evidence of interaction with a non-classical squeezed reservoir.

Based on established circuit QED techniques from Refs. [57,58,65], the proposed squeezed-reservoir QB is ex-

perimentally feasible. A transmon qubit embedded in a JPA can serve as the QB, with the JPA generating the required broadband squeezed vacuum reservoir when flux-pumped in the degenerate mode. This integrated approach, similar to the qubit-parametric-amplifier (QPA) architecture in Ref. [57], enables both generation of the engineered squeezed reservoir and high-efficiency measurement of the QB's energy and ergotropy. The predicted nonmonotonic ergotropy versus squeezing strength can be systematically tested by tuning the JPA pump power and phase, analogous to existing squeezing protocols for controlling dephasing and measurement sensitivity.[57,58,65] While challenges such as parasitic dephasing from on-chip squeezing and saturation effects exist, they can be mitigated through device optimization, making this a viable platform for exploring quantum-enhanced energy storage.

In summary, squeezed-vacuum reservoir engineering, implemented via a parametrically controlled broadband squeezed laser driving a QB-embedded cavity-QED system, significantly optimizes QB performance. By deriving a reduced master equation through the adiabatic elimination method, we reveal that the squeezing parameters govern both the energy-transfer dynamics and the ergotropy of the QB. Increasing the squeezing strength enhances the charging rate, enabling rapid energy transfer, while the steady-state energy saturates beyond critical squeezing parameters.

A key finding is the nonmonotonic dependence of ergotropy on squeezing strength: it peaks at an optimal squeezing parameter before declining, indicating a trade-off between squeezing-enhanced QB–charger coupling and squeezing-induced amplified dissipation. This identifies an experimentally tunable regime where squeezed-reservoir engineering maximizes ergotropy, offering a resource-efficient strategy for enhancing quantum energy storage devices. Our results may stimulate further experimental and theoretical investigations into controllable quantum resources for optimizing QB efficiency. This work demonstrates how quantum squeezing effects can be utilized to enhance the performance of quantum thermodynamic devices. The identified mechanism provides a pathway to exploit quantum reservoir engineering to optimize QB performance in open quantum systems.

Acknowledgments

This project is supported by the National Natural Science Foundation of China (Grants No. 12274422) and the Natural Science Foundation of Hubei Province (Grant No. 2022CFA013). J.-B. Y. acknowledges support from A*STAR (Grant Nos. C230917003 and C230917007) and Q.InC Strategic Research and Translational Thrust.

References

[1] Alicki R and Fannes M 2013 *Phys. Rev. E* **87** 042123
[2] Ferraro D, Campisi M, Andolina G M, Pellegrini V and Polini M 2018 *Phys. Rev. Lett.* **120** 117702
[3] Pokhrel S and Gea-Banacloche J 2025 *Phys. Rev. Lett.* **134** 130401
[4] Dou F Q, Zhou H and Sun J A 2022 *Phys. Rev. A* **106** 032212
[5] Li Y L, Liao C H and Xiao X 2025 *Chin. Phys. B* **34** 010307
[6] Liu F, Yang H Y, Wang S L, Wang J Z, Zhang K and Wang X H 2025 *Chin. Phys. B* **34** 020306
[7] Yu W L, Zhang Y, Li H, Wei G F, Han L P, Tian F and Zou J 2023 *Chin. Phys. B* **32** 010302
[8] Andolina G M, Keck M, Mari A, Campisi M, Giovannetti V and Polini M 2019 *Phys. Rev. Lett.* **122** 047702
[9] Gyhm J Y, Šafránek D and Rosa D 2022 *Phys. Rev. Lett.* **128** 140501
[10] Rossini D, Andolina G M, Rosa D, Carrega M and Polini M 2020 *Phys. Rev. Lett.* **125** 236402
[11] Song W L, Liu H B, Zhou B, Yang W L and An J H 2024 *Phys. Rev. Lett.* **132** 090401
[12] Song W L, Wang J L, Zhou B, Yang W L and An J H 2025 *Phys. Rev. Lett.* **135** 020405
[13] Farina D, Andolina G M, Mari A, Polini M and Giovannetti V 2019 *Phys. Rev. B* **99** 035421
[14] Julià-Farré S, Salamon T, Riera A, Bera M N and Lewenstein M 2020 *Phys. Rev. Res.* **2** 023113
[15] Abah O, De Chiara G, Paternostro M and Puebla R 2022 *Phys. Rev. Res.* **4** L022017
[16] Kamin F H, Tabesh F T, Salimi S and Santos A C 2020 *Phys. Rev. E* **102** 052109
[17] Shi H L, Ding S, Wan Q K, Wang X H and Yang W L 2022 *Phys. Rev. Lett.* **129** 130602
[18] Wang L, Liu S Q, Wu F l, Fan H and Liu S Y 2023 *Phys. Rev. A* **108** 062402
[19] Sen K and Sen U 2021 *Phys. Rev. A* **104** L030402
[20] Imai S, Gühne O and Nimmrichter S 2023 *Phys. Rev. A* **107** 022215
[21] Centrone F, Mancino L and Paternostro M 2023 *Phys. Rev. A* **108** 052213
[22] Hovhannisyan K V, Perarnau-Llobet M, Huber M and Acín A 2013 *Phys. Rev. Lett.* **111** 240401
[23] Monsel J, Fellous-Asiani M, Huard B and Auffèves A 2020 *Phys. Rev. Lett.* **124** 130601
[24] Santos A C, Çakmak B, Campbell S and Zinner N T 2019 *Phys. Rev. E* **100** 032107
[25] Binder F C, Vinjanampathy S, Modi K and Goold J 2015 *New J. Phys.* **17** 075015
[26] Le T P, Levinsen J, Modi K, Parish M M and Pollock F A 2018 *Phys. Rev. A* **97** 022106
[27] Campaioli F, Pollock F A, Binder F C, Céleri L, Goold J, Vinjanampathy S and Modi K 2017 *Phys. Rev. Lett.* **118** 150601
[28] Arjmandi M B, Shokri A, Faizi E and Mohammadi H 2022 *Phys. Rev. A* **106** 062609
[29] Crescente A, Carrega M, Sassetti M and Ferraro D 2020 *Phys. Rev. B* **102** 245407
[30] Andolina G M, Keck M, Mari A, Giovannetti V and Polini M 2019 *Phys. Rev. B* **99** 205437
[31] Dou F Q, Lu Y Q, Wang Y J and Sun J A 2022 *Phys. Rev. B* **105** 115405
[32] Skrzypczyk P, Short A J and Popescu S 2014 *Nat. Commun.* **5** 4185
[33] Zhang Y Y, Yang T R, Fu L and Wang X 2019 *Phys. Rev. E* **99** 052106
[34] Chang W, Yang T R, Dong H, Fu L, Wang X and Zhang Y Y 2021 *New J. Phys.* **23** 103026
[35] Quach J Q, McGhee K E, Ganzer L, Rouse D M, Lovett B W, Gauger E M, Keeling J, Cerullo G, Lidzey D G and Virgili T 2022 *Sci. Adv.* **8** eabk3160
[36] Hu C K, Qiu J, Souza P J P, Yuan J, Zhou Y, Zhang L, Chu J, Pan X, Hu L, Li J, Xu Y, Zhong Y, Liu S, Yan F, Tan D, Bachelard R, Villas-Boas C J, Santos A C and Yu D 2022 *Quantum Sci. Technol.* **7** 045018
[37] Joshi J and Mahesh T S 2022 *Phys. Rev. A* **106** 042601
[38] Gemme G, Grossi M, Ferraro D, Vallecorsa S and Sassetti M 2022 *Batteries* **8** 43
[39] Zheng R H, Ning W, Yang Z B, Xia Y and Zheng S B 2022 *New J. Phys.* **24** 063031
[40] Yu J, Wang S, Liu K, Zha C, Wu Y, Chen F, Ye Y, Li S, Zhu Q, Guo S, Qian H, Huang H L, Zhao Y, Ying C, Fan D, Wu D, Su H, Deng H, Rong H, Zhang K, Cao S, Lin J, Xu Y, Guo C, Li N, Liang F, Wu G, Huo Y H, Lu C Y, Peng C Z, Nemoto K, Munro W J, Zhu X, Pan J W and Gong M 2024 *Phys. Rev. A* **109** 062614

[41] Huang X, Wang K, Xiao L, Gao L, Lin H and Xue P 2023 *Phys. Rev. A* **107** L030201
[42] Qu D, Zhan X, Lin H and Xue P 2023 *Phys. Rev. B* **108** L180301
[43] Zhu G, Chen Y, Hasegawa Y and Xue P 2023 *Phys. Rev. Lett.* **131** 240401
[44] Maillette de Buy Wenniger I, Thomas S E, Maffei M, Wein S C, Pont M, Belabas N, Prasad S, Harouri A, Lemaître A, Sagnes I, Somaschi N, Auffèves A and Senellart P 2023 *Phys. Rev. Lett.* **131** 260401
[45] Zhang J, Wang P, Chen W, Cai Z, Qiao M, Li R, Huang Y, Tian H, Tu H, Cui K, Yan L, Zhang J, Zhang J, Yung M and Kim K 2025 *Phys. Rev. Lett.* **135** 140403
[46] Dou F Q and Yang F M 2023 *Phys. Rev. A* **107** 023725
[47] Delmonte A, Crescente A, Carrega M, Ferraro D and Sassetti M 2021 *Entropy* **23** 612
[48] Yang D L, Yang F M and Dou F Q 2024 *Phys. Rev. B* **109** 235432
[49] Downing C A and Ukhtary M S 2023 *Commun. Phys.* **6** 322
[50] Downing C A and Ukhtary M S 2024 *Phys. Rev. A* **109** 052206
[51] Konar T K, Patra A, Gupta R, Ghosh S and SenDe A 2024 *Phys. Rev. A* **110** 022226
[52] Downing C and Ukhtary M 2024 *Phys. Lett. A* **518** 129693
[53] Georgiades N P, Polzik E S, Edamatsu K, Kimble H J and Parkins A S 1995 *Phys. Rev. Lett.* **75** 3426
[54] Wang Y D and Clerk A A 2013 *Phys. Rev. Lett.* **110** 253601
[55] Kimchi-Schwartz M E, Martin L, Flurin E, Aron C, Kulkarni M, Tureci H E and Siddiqi I 2016 *Phys. Rev. Lett.* **116** 240503
[56] Zeytinoğlu S, İmamoğlu A M C and Huber S 2017 *Phys. Rev. X* **7** 021041
[57] Eddins A, Kreikebaum J M, Toyli D M, Levenson-Falk E M, Dove A, Livingston W P, Levitan B A, Govia L C G, Clerk A A and Siddiqi I 2019 *Phys. Rev. X* **9** 011004
[58] Bienfait A, Campagne-Ibarcq P, Kiilerich A H, Zhou X, Probst S, Pla J J, Schenkel T, Vion D, Esteve D, Morton J J L, Moelmer K and Bertet P 2017 *Phys. Rev. X* **7** 041011
[59] Kraus B and Cirac J I 2004 *Phys. Rev. Lett.* **92** 013602
[60] Yang C J, An J H, Yang W and Li Y 2015 *Phys. Rev. A* **92** 062311
[61] Liu R and An J H 2025 *Phys. Rev. A* **111** 043718
[62] Hou Q Z, You J B, Yang W L, An J H, Chen C Y and Feng M 2018 *Opt. Express* **26** 20459
[63] Bai S Y and An J H 2021 *Phys. Rev. Lett.* **127** 083602
[64] Carmichael H J, Lane A S and Walls D F 1987 *Phys. Rev. Lett.* **58** 2539
[65] Toyli D M, Eddins A W, Boutin S, Puri S, Hover D, Bolkhovsky V, Oliver W D, Blais A and Siddiqi I 2016 *Phys. Rev. X* **6** 031004
[66] Clark J B, Lecocq F, Simmonds R W, Aumentado J and Teufel J D 2017 *Nature* **541** 191
[67] Wilson-Rae I, Nooshi N, Zwerger W and Kippenberg T J 2007 *Phys. Rev. Lett.* **99** 093901
[68] Cirac J I, Blatt R, Zoller P and Phillips W D 1992 *Phys. Rev. A* **46** 2668
[69] Cirac J I 1992 *Phys. Rev. A* **46** 4354
[70] Zhou P and Swain S 1998 *Phys. Rev. A* **58** 1515
[71] Manzano G 2018 *Phys. Rev. E* **98** 042123
[72] Polzik E S 2008 *Nature* **453** 45
[73] Shen H Z, Shang C, Zhou Y H and Yi X X 2018 *Phys. Rev. A* **98** 023856
[74] Shen H Z, Wang Q, Wang J and Yi X X 2020 *Phys. Rev. A* **101** 013826
[75] Shen H Z, Yang J F and Yi X X 2024 *Phys. Rev. A* **109** 043714
[76] Vacchini B and Breuer H P 2010 *Phys. Rev. A* **81** 042103
[77] Breuer H P, Laine E M and Piilo J 2009 *Phys. Rev. Lett.* **103** 210401
[78] Shen H Z, Xu S, Cui H T and Yi X X 2019 *Phys. Rev. A* **99** 032101
[79] Yang W L, An J H, Zhang C, Feng M and Oh C H 2013 *Phys. Rev. A* **87** 022312